

First High-speed Camera Observations of the Optical Counterpart of a Terrestrial Gamma-ray Flash

R.U. Abbasi,^{1,*} J.W.Belz,² M. M. F. Saba,³ P. R. Krehbiel,⁴ J. Remington,^{2,5} M. A. Stanley,⁴ D. R. da Silva,³ W. Rison,⁴ Dan Rodeheffer,⁴ N. Kieu,¹ J. Mazich,¹ R. LeVon,² K. Smout,² A. Petrizze,² for the Telescope Array Collaboration,^{6,7} T. Abu-Zayyad,^{6,7} M. Allen,⁶ Y. Arai,⁸ R. Arimura,⁸ E. Barcikowski,⁶ D.R. Bergman,⁶ S.A. Blake,⁶ I. Buckland,⁶ B.G. Cheon,⁹ M. Chikawa,¹⁰ T. Fujii,¹¹ K. Fujisue,¹⁰ K. Fujita,⁸ R. Fujiwara,⁸ M. Fukushima,¹⁰ G. Furlich,⁶ N. Globus,^{12,†} R. Gonzalez,⁶ W. Hanlon,⁶ N. Hayashida,¹³ H. He,¹² K. Hibino,¹³ R. Higuchi,¹⁰ K. Honda,¹⁴ D. Ikeda,¹³ N. Inoue,¹⁵ T. Ishii,¹⁴ H. Ito,¹² D. Ivanov,⁶ H. Iwakura,¹⁶ A. Iwasaki,⁸ H.M. Jeong,¹⁷ S. Jeong,¹⁷ C.C.H. Jui,⁶ K. Kadota,¹⁸ F. Kakimoto,¹³ O. Kalashev,¹⁹ K. Kasahara,²⁰ S. Kasami,²¹ S. Kawakami,⁸ K. Kawata,¹⁰ I. Kharuk,¹⁹ E. Kido,¹² H.B. Kim,⁹ J.H. Kim,^{6,‡} J.H. Kim,⁶ S.W. Kim,¹⁷ Y. Kimura,⁸ I. Komae,⁸ Y. Kubota,¹⁶ V. Kuzmin,^{19,§} M. Kuznetsov,^{22,19} Y.J. Kwon,²³ K.H. Lee,¹⁷ B. Lubsandorzhiev,¹⁹ J.P. Lundquist,^{24,6} H. Matsumiya,⁸ T. Matsuyama,⁸ J.N. Matthews,⁶ R. Mayta,⁸ I. Myers,⁶ S. Nagataki,¹² K. Nakai,⁸ R. Nakamura,¹⁶ T. Nakamura,²⁵ T. Nakamura,¹⁶ Y. Nakamura,¹⁶ A. Nakazawa,¹⁶ E. Nishio,²¹ T. Nonaka,¹⁰ H. Oda,⁸ S. Ogio,¹⁰ M. Ohnishi,¹⁰ H. Ohoka,¹⁰ Y. Oku,²¹ T. Okuda,²⁶ Y. Omura,⁸ M. Ono,¹² A. Oshima,²⁷ S. Ozawa,²⁸ I.H. Park,¹⁷ M. Potts,^{6,¶} M.S. Pshirkov,^{19,29} J. Remington,⁶ D.C. Rodriguez,⁶ C. Rott,^{6,17} G.I. Rubtsov,¹⁹ D. Ryu,³⁰ H. Sagawa,¹⁰ N. Sakaki,¹⁰ T. Sako,¹⁰ N. Sakurai,⁸ K. Sato,⁸ T. Seki,¹⁶ K. Sekino,¹⁰ P.D. Shah,⁶ Y. Shibasaki,¹⁶ N. Shibata,²¹ T. Shibata,¹⁰ J. Shikita,⁸ H. Shimodaira,¹⁰ B.K. Shin,³⁰ H.S. Shin,¹⁰ D. Shinto,²¹ J.D. Smith,⁶ P. Sokolsky,⁶ B.T. Stokes,⁶ T.A. Stroman,⁶ K. Takahashi,¹⁰ M. Takamura,³¹ M. Takeda,¹⁰ R. Takeishi,¹⁰ A. Taketa,³² M. Takita,¹⁰ Y. Tamada,²¹ K. Tanaka,³³ M. Tanaka,³⁴ Y. Tanoue,⁸ S.B. Thomas,⁶ G.B. Thomson,⁶ P. Tinyakov,^{22,19} I. Tkachev,¹⁹ H. Tokuno,³⁵ T. Tomida,¹⁶ S. Troitsky,¹⁹ R. Tsuda,⁸ Y. Tsunesada,^{8,36} S. Udo,¹³ T. Uehama,¹⁶ F. Urban,³⁷ D. Warren,¹² T. Wong,⁶ M. Yamamoto,¹⁶ K. Yamazaki,²⁷ K. Yashiro,³¹ F. Yoshida,²¹ Y. Zhezher,^{10,19} and Z. Zundel¹⁶

¹Department of Physics, Loyola University Chicago, Chicago, Illinois, USA

²Department of Physics and Astronomy, University of Utah, Salt Lake City, Utah, USA

³National Institute for Space Research (INPE), São José dos Campos, Brazil

⁴Langmuir Laboratory for Atmospheric Research,

New Mexico Institute of Mining and Technology, Socorro, NM, USA

⁵NASA Marshall Space Flight Center, Huntsville, Alabama, USA

⁶High Energy Astrophysics Institute and Department of Physics and Astronomy,
University of Utah, Salt Lake City, Utah 84112-0830, USA

⁷Department of Physics, Loyola University Chicago, Chicago, Illinois 60660, USA

⁸Graduate School of Science, Osaka Metropolitan University, Sugimoto, Sumiyoshi, Osaka 558-8585, Japan

⁹Department of Physics and The Research Institute of Natural Science,
Hanyang University, Seongdong-gu, Seoul 426-791, Korea

¹⁰Institute for Cosmic Ray Research, University of Tokyo, Kashiwa, Chiba 277-8582, Japan

¹¹The Hakubi Center for Advanced Research and Graduate School of Science,
Kyoto University, Kitashirakawa-Oiwakecho, Sakyo-ku, Kyoto 606-8501, Japan

¹²Astrophysical Big Bang Laboratory, RIKEN, Wako, Saitama 351-0198, Japan

¹³Faculty of Engineering, Kanagawa University, Yokohama, Kanagawa 221-8686, Japan

¹⁴Interdisciplinary Graduate School of Medicine and Engineering,
University of Yamanashi, Kofu, Yamanashi 400-8511, Japan

¹⁵The Graduate School of Science and Engineering,
Saitama University, Saitama, Saitama 338-8570, Japan

¹⁶Academic Assembly School of Science and Technology Institute of Engineering,
Shinshu University, Nagano, Nagano 380-8554, Japan

¹⁷Department of Physics, SungKyunKwan University, Jang-an-gu, Suwon 16419, Korea

¹⁸Department of Physics, Tokyo City University, Setagaya-ku, Tokyo 158-8557, Japan

¹⁹Institute for Nuclear Research of the Russian Academy of Sciences, Moscow 117312, Russia

²⁰Faculty of Systems Engineering and Science, Shibaura Institute of Technology, Minato-ku, Tokyo 337-8570, Japan

²¹Department of Engineering Science, Faculty of Engineering,
Osaka Electro-Communication University, Neyagawa-shi, Osaka 572-8530, Japan

²²Service de Physique Théorique, Université Libre de Bruxelles, Brussels 1050, Belgium

²³Department of Physics, Yonsei University, Seodaemun-gu, Seoul 120-749, Korea

²⁴Center for Astrophysics and Cosmology, University of Nova Gorica, Nova Gorica 5297, Slovenia

²⁵Faculty of Science, Kochi University, Kochi, Kochi 780-8520, Japan

²⁶Department of Physical Sciences, Ritsumeikan University, Kusatsu, Shiga 525-8577, Japan

²⁷College of Engineering, Chubu University, Kasugai, Aichi 487-8501, Japan

²⁸Quantum ICT Advanced Development Center, National Institute for

Information and Communications Technology, Koganei, Tokyo 184-8795, Japan

²⁹Sternberg Astronomical Institute, Moscow M.V. Lomonosov State University, Moscow 119991, Russia

³⁰Department of Physics, School of Natural Sciences,

Ulsan National Institute of Science and Technology, UNIST-gil, Ulsan 689-798, Korea

³¹Department of Physics, Tokyo University of Science, Noda, Chiba 162-8601, Japan

³²Earthquake Research Institute, University of Tokyo, Bunkyo-ku, Tokyo 277-8582, Japan

³³Graduate School of Information Sciences, Hiroshima City University, Hiroshima, Hiroshima 731-3194, Japan

³⁴Institute of Particle and Nuclear Studies, KEK, Tsukuba, Ibaraki 305-0801, Japan

³⁵Graduate School of Science and Engineering, Tokyo Institute of Technology, Meguro, Tokyo 152-8550, Japan

³⁶Nambu Yoichiro Institute of Theoretical and Experimental Physics,

Osaka Metropolitan University, Sugimoto, Sumiyoshi, Osaka 558-8585, Japan

³⁷CEICO, Institute of Physics, Czech Academy of Sciences, Prague 182 21, Czech Republic

In this paper, we present the first observation of optical emission of a downward-directed terrestrial gamma ray flash (TGF). The optical emission was observed by a high-speed video camera Phantom v2012 in conjunction with the Telescope Array (TA) surface detector, lightning mapping array, interferometer, fast antenna, and the national lightning detection network. The suite of gamma and lightning instruments, timing resolution, and source proximity offers us an unprecedented look at the TGF phenomena. On September 11 of 2021 we observed a storm above the TA detector. The storm resulted in six extremely energetic TGF events that were produced by flashes with return stroke peak currents up to 223 kA. The observed TGFs were found to correlate directly to the initial burst pulse signal of the lightning flash while producing an intense optical signature. Results from this study allow us to further the understanding regarding the initiation mechanism of TGFs.

I. INTRODUCTION

Terrestrial Gamma-ray Flashes (TGFs) are bursts of gamma-ray radiation produced via bremsstrahlung in the Earth's atmosphere. TGFs were first observed by the Burst and Transient Source Experiment (BATSE) on the Compton Gamma-Ray Observatory satellite [1, 2]. Since then, satellite experiments (e.g. RHESSI [3, 4], Fermi [5], AGILE [6], ASIM [7]) have detected thousands of TGFs, demonstrating that TGFs are produced by lightning flashes. In particular, the observations show that TGFs occur within the first few milliseconds of upward intra-cloud (IC) flashes [7–13]. Even though thousands of TGFs seem to be produced inside thunderstorms [1–7], the mechanism responsible for producing them and how IC discharges relate to TGFs is still unknown.

The leading mechanism that produces TGFs is believed to be the Relativistic Runaway Electron Avalanche (RREA) [14]. RREA is described by a multiplication process through high-energy, electron-electron elastic scattering (primarily Møller scattering). RREA is responsible for the acceleration and the multiplication of seed electrons in thunderstorms under high electric fields. Dwyer 2008 [15] showed that the high number of electrons required to produce a TGF cannot be explained

by the steady state of background radiation nor by the extensive air showers from cosmic rays. The two main theories that were developed to interpret the high-fluence TGF observations are the Relativistic FeeDback mechanism (RFD) [16] and the the lightning leader models also called the thermal runaway mechanism [17].

The Relativistic FeeDback (RFD) mechanism, introduced by Dwyer in 2003 [16], suggests that photons and positrons produce feedback that exponentially increases the number of runaway electron avalanches. In this model, Dwyer includes the production of photons via Compton backscattering of x -rays from the runaway electrons. The backscattered photons propagate backward to the region of the avalanche with a high electric field, producing other runaway electrons via Compton scattering of photoelectric absorption. The relativistic feedback mechanism model also includes the production of positrons created via pair production of gamma rays. The positrons, like high-energy photons, also return back to the initial position of the avalanche, producing further avalanches. With the relativistic feedback method, in a timescale of a few microseconds, the number of avalanches produced is enough to explain TGF observations and can produce the needed energetic electrons.

The thermal runaway electron's production mechanism, on the other hand, assumes a localized high electric field (Ten times larger than the conventional breakdown field) [18]. The thermal runaway electron's production mechanism assumes that TGF events are produced in the vicinity of the tips of streamers related to lightning leaders. The free electron population is then accelerated further in the potential drops in front of lightning leader tips to runaway electrons via the thermal runaway mechanism [17, 19].

Both runaway electron production models, are tuned

* rabbasi@luc.edu

† Presently at: University of California - Santa Cruz and Flatiron Institute, Simons Foundation

‡ Presently at: Argonne National Laboratory, Physics Division, Lemont, Illinois 60439, USA

§ Deceased

¶ Presently at: Georgia Institute of Technology, Physics Department, Atlanta, Georgia 30332, USA

to interpret TGF spectrum measurements and large fluxes observed by satellite and ground detectors. Both models have been successful in describing the satellite TGF's observed spectrum and fluence. The optical emission of TGFs, on the other hand, would provide definitive evidence as to which of the production and propagation models is responsible for TGFs observations [18]. Moreover, the intensities at which the optical emission wavelengths are detected provide key information of the lightning development sequence. If TGFs are produced through *thermal runaway electrons* in streamers, then this discharge should produce an optical signal before or simultaneously with the production of gamma emission. If TGFs are byproducts of *relativistic feedback discharges*, and because they do not involve a leader channel, they will emit high-current electric discharge that generate radio emissions similar to lightning. However, this radio emission produce light in the UV lines and little to no emission in the visible range compared to lightning. This is also referred to as "dark lightning" [20].

Previous downward-directed Terrestrial Gamma-ray Flashes (TGFs) observations, using the 700 km^2 Telescope Array Surface Detector (TASD), established that observed lightning-correlated energetic particles are downward-directed gamma-ray showers. Moreover, these downward-directed gamma-ray showers were found to be correlated with the early leader [21] and the initial burst pulse [22] stage of cloud-to-ground lightning. In this work, we use the TASD detector, together with a high-speed video camera, in conjunction with the suite of lightning instruments at the TASD site, to report on the optical emission of downward-directed terrestrial gamma ray flashes. The optical emission observations should allow us to better understand which runaway electron production model is responsible for gamma-ray production in the atmosphere.

II. INSTRUMENTATION

The observations of downward-directed TGFs, reported in this work, were detected by the large-area Telescope Array cosmic ray observatory (TADS) located in the southwestern desert of Utah. The flashes that produced the TGFs were recorded simultaneously by a high-speed video camera, a Lightning Mapping Array (LMA), a broadband VHF interferometer, and Fast Antenna (FA). Figure 4 (provided in the supplementary information) shows the layout of all of the involved detectors. Each of these detectors is described in detail in [21], [22], [23], and [24], except the recently installed high-speed video camera. In this section, we will introduce each of these instruments briefly.

The **Telescope Array Surface Detector (TASD)** is a ground-based surface detector primarily designed to observe Ultra High Energy Cosmic Rays (UHECR). With an area coverage of 700 km^2 the TASD is the largest UHECR detector in the Northern Hemisphere. It com-

prises of 507 scintillator detectors (SDs). Each SDs unit consists of upper and lower scintillator planes. Each plane is 3 m^2 in area and 1.2 cm in thickness, separated by a 1 mm thick stainless-steel sheet. Each plane is read out by individual photomultiplier tubes via wavelengths shifting fiber. The output signals from the photomultipliers is digitized with a 50 MHz sampling rate. Each SD is housed inside an RF-sealed and light-tight stainless-steel enclosure. An event trigger occurs when three adjacent TASDs observe a time-integrated signal greater than 3 Vertical Equivalent Muons (VEMs) within $8 \mu\text{s}$ (Note that 1 VEM deposits an energy of $\sim 2.1 \text{ MeV}$). When an event trigger occurs, the signals from all individually triggered SDs within $\pm 32 \mu\text{s}$ are recorded [21, 23]. The TASD detector observed approximately 25 downward-directed Terrestrial Gamma-ray Flashes (TGFs) within the past 13 years, making it the world leading detector in downward-directed TGF observations. Details of the detector's design, trigger, particle-energy can be found in [21–23].

The **High-speed video camera** is a monochrome Phantom V2012 operating at 40,000 frames per second with time interval between frames of $25.00 \mu\text{s}$ and exposure time of $23.84 \mu\text{s}$ (at the end of each frame the camera is blind for $1.14 \mu\text{s}$ due to data transfer). Each frame of the video is time stamped by means of a GPS antenna and has a resolution of 1280×448 pixels. The camera is sensitive in the visible and the near-infrared spectra (400 nm - 1000 nm). The camera was installed ten kilometers to the east border of the TASD inside a building adjacent to the INTF and the FA. The 20-mm focal length lens allowed a vertical viewing angle of 35 degrees, and a horizontal angle of 84 degrees covering almost all of the TASD detectors. The camera's position and settings were optimized to observed downward TGF sources that are approximately within 30 km from the camera and up to 3 km above ground level. Each video had a recording length of 1.1 seconds and was automatically triggered by changes in luminosity. Data from the camera is saved on a computer at the site and analyzed offline. The elevation angles from the camera together with the LMA were used to calculate the source altitude of the TGFs.

The **Lightning Mapping Array (LMA)**, developed by the Langmuir Laboratory group at New Mexico Tech [25, 26], has been running at the TASD detector since 2013. The LMA detects the lightning sources emitting an impulse signal emission between 60MHz -66MHz. LMA detected sources are analyzed using the time-of-arrival technique of the impulse signal time for multiple triggered LMA stations on the ground. This technique provides us with detailed 3D images of the VHF radiation produced by the lightning inside storms. The LMA detects VHF with a time accuracy of 35-ns root mean square over a wide ($> 70 \text{ dB}$) dynamic range, from $\leq 10 \text{ mW}$ to $> 100 \text{ kW}$ peak source power. Cell data modems connect each station into the internet, allowing decimated data to be processed in real time and posted

on the web, and for monitoring station operation.

The **INTerFerometer (INTF)** and the **Fast electric field change Antenna (FA)** at the TASD site. The INTF records broadband (20 - 80 MHz) waveforms at 180 MHz from three flat-plate receiving antennas. The three antennas were positioned in a triangular baseline of 106–121 m. Such a baseline was used to maximize the angular resolution over the TASD detector. The INTF is processed offline to determine the two-dimensional azimuth and elevation arrival directions of the VHF radiation with sub-microsecond resolution [27]. The FA, on the other hand, records the electric field changes of lightning discharges. The FA is continuously recording at high resolution 180 MHz measurements of the LF/ELF discharge sferics. This is using a downward looking flat plate sensor with data stored locally on an SD card and processed offline as well.

III. OBSERVATIONS

After the installation of the high-speed video camera on August 12, 2021, we recorded several lightning flashes over the TASD before detecting the first optical observations of downward-directed TGF events on September 11, 2021. On that day nine flashes occurred over the TASD detector. They were all cloud-to-ground flashes with negative polarity. Six of these nine flashes produced TGFs, all of them occurring during a time interval of only 51 minutes. The three non-producing TGF flashes had return strokes peak current less than 36 kA. The six-gamma ray initiating flashes, on the other hand, were produced by flashes with peak current greater than 51 kA. In all the TGF producing flashes that had multiple return strokes (four of them), the TGF was associated with the first return stroke. In all the multiple return stroke flashes, the subsequent strokes made different ground contact points and the first return stroke was the most intense.

While the Telescope Array detector has observed over 25 TGFs in the last 13 years, this weakly convective, hail producing (as reported by scientists from the site) storm, in particular, has been found to be special in many ways. At first, all the TGFs observed on that day were produced by cloud-to-ground flashes with return stroke peak currents that ranged in magnitude from 53 kA all the way to 223 kA. In addition, the maximum energy deposit on one of the surface detectors had reached energies of up to 33,913 VEM (74 GeV). Also, the duration of the observed TGFs had reached up to 719 μ s. Note that all of the previously detected TGFs by the TASD detector, except for flash three in [21], were produced by flashes with an average peak current of 52 kA and maximum peak current of 139 kA, a deposited maximum energy on a single surface detector of no more than 997 VEM (2 GeV) and a duration of less than 551 μ s.

Most importantly, while the average rate of TGF observations by the TASD detector has varied from one to two events per year, this storm resulted in six TGF ob-

servations within one hour (25% of all TGF observed in the past 13 years). This makes it the highest rate of TGF observations in both one thunderstorm and in all thunderstorm seasons observed by the TASD detector in the southwestern desert of Utah.

While we observed six flashes on September 11 of 2021, we will focus and make a more detailed analysis of the fourth flash observed on 17:11:12 UTC by the TASD, the high-speed video camera, INTF, and FA. We chose this event because it was the clearest and the most straightforward to analyze. This TGF resulted in three bursts of gamma ray triggers reported by the TASD detector. We will refer to these triggers as trigger A, B, and C. The gamma footprint on the ground for this TGF is shown in Figure 5 in the supplementary information. As shown in the figure, the maximum size of the TGF footprint on the ground, as observed by the TASD, is approximately 6 km in diameter. The maximum energy deposited in a TASD detector was 1.8 GeV. The TGF burst lasted for 719 microseconds and was followed by a high peak current return stroke of -154 kA as reported by the National Lightning Detection Network (NLDN).

The fourth's TGF burst A, B, and C trigger sources were produced close to the most eastward part of the TASD detector with a 10.9 km distance from the high-speed video camera, INTF, and FA location. Trigger A, B, and C source heights were analyzed using two independent analyses and were found to be consistent within uncertainties. The first method used the camera and LMA and the second used the INTF and LMA. In the case of the camera, the heights were found using the camera pointing direction and the LMA longitude and latitude locations of 2.5 km, 1.9 km, and 1.3 km above ground level \pm 10 % uncertainty. In the case of the second method, the heights were found using the INTF elevation and azimuthal direction together with LMA longitude and latitude locations [21] to be 2.4 km, 1.9 km, and 1.4 km above ground level \pm 10 % uncertainty. Moreover, the propagation speed of the leader at trigger A, B, C was found to be 7.2×10^6 m/s, 2.5×10^6 m/s, and 3.0×10^6 m/s respectively. Figure 1 shows the lightning flash and the height, elevation, and azimuth of the trigger A, B, C sources as observed by the high-speed video camera, the INTF, and the TASD detectors.

Figure 2 shows the progression of the leader of this flash in multiple selected frames as observed by the high-speed video camera. Some of the selected frames display a light saturation problem. This problem is due to the fact the camera's settings were conservatively optimized for suspected multiple scenarios including a very faint signal if the sources of the TGFs were inside the cloud and would suffer from light scattering. The initial camera settings would have, in principle, allowed us to detect possible faint signals due to scattering or absorption for up to 30 kilometers away. However, this TGF storm was not only the most energetic TGF producing thunderstorm we have ever observed, but the leaders that produced TGFs was also well developed, very intense and below cloud

base when the TGF bursts occurred. Their intense luminosity and speed reveal a high density charged leader. In some cases (trigger B and C) the leaders were even close to half-way to the ground as shown in Figure 1.

Figure 3 combines the TASD, high-speed video camera luminosity, INTF, and the FA observations. The time delay in each of these figures are removed using the temporal comparison method discussed in [22]. Two different zooms of this flash are displayed. Figure 3-top plot shows the detectors' observations within 3 milliseconds, while Figures 2-bottom plot shows a one millisecond zoom. The TASD, INTF, and FA data displayed in this plot are both triggered and analyzed similarly to previous TGFs we reported on in [22]. The luminosity curve, on the other hand, shown in dark blue is measured by averaging the diffused luminosity in the pixels in the image. The pixels used are adjacent to the lightning flash instead of the pixels including the flash itself. An example of this luminosity calculation is shown in the last snapshot in Figure 2. The pixels used in calculating the luminosity for this snapshot are contained in the green box displayed next to the flash. The luminosity is calculated by summing over all the pixels intensity values, inside the green box, and then dividing it by the total number of pixels. The motivation behind this method is to avoid misleading peaks in the luminosity (possible plateaus) that could have been encountered due to the saturation in the luminosity shown in several snapshots in Figure 2. Note that we did compare both the average luminosity including the adjacent pixels to the flash vs. the pixels including the flash itself and found that both intensity curves are consistent with each other for this flash.

IV. DISCUSSION AND CONCLUSION

This work examines the luminosity of an extremely energetic downward-direct terrestrial gamma-ray produced in a cloud-to-ground flash. This TGF presented unique features in terms of energy deposit, duration, and was correlated with a very high peak current return stroke. In recent years, Energetic In-cloud Pulses (EIP) generating lightning flashes have been concluded to produce a class of satellite directed TGFs. One of the main characteristics of EIPs is the production of extremely energetic events with a high peak current greater than 150 kA [28]. It is interesting to note that the TGF sources, reported in this work, produced in this rare thunderstorm, are found to correlate with an initial breakdown pulse and an extremely energetic thunderstorm that corresponds in peak current magnitude to EIPs. It is also interesting to note that the fluence of this flash was found to be 3×10^{15} which is also comparable to the lower limit fluence estimates for TGF satellite observations.

The energetic observed gamma ray bursts were produced as the leader clearly formed below the cloud base, in some bursts more than half-way to the ground. The

downward atmospheric gamma ray consisted of isolated bursts that are clearly correlated with initial breakdown (IB) pulses. The optical luminosity observed for these TGFs start to increase within 25 μ s from the onset of the IBP and the TGF signal and continues to increase 25-50 μ s after TGF and IBP signal ceases. In total, the intensity of the entire optical emission duration lasts between 50-100 μ s.

The TGF timing relative to the E-change pulses and the visible light emission is crucial to our understanding of their initiation and propagation. Our data indicate a substantial increase in the visible light in correlation with the TGF production. From this result it seems reasonable to conclude that our result supports the thermal runaway mechanism model and does not support the idea that TGFs are dark events as proposed by Relativistic FeedBack mechanism.

The state-of-the-art satellite ASIM have revealed in the past two years, for the first time and, with high timing accuracy, the optical emission timing and strength in relationship to TGFs and Transient Luminous Events (TLE) observations. The Modular Multi-spectral Imaging Array (MMIA) on-board the ASIM satellite, is made of high-speed photometers at 337 nm, and 777.4 nm (both used for detecting lightning) with a 100 kHz sampling rate [7].

A consistent feature of ASIM satellite's optical emission observations is that the TGFs were observed one to two ms after the beginning of a weak increase in the optical emission in the 337 nm and 777.4 nm photometers, and before the onset of the main optical pulse. Such observations indicates that the optical emission and the upward observed TGFs have the same source.

Similarly results from this work, using the high-speed video camera in conjunction with the TASD detector and a suite of lightning instruments, supports the satellite-based measurements by ASIM. To further compare the optical signature of downward and upward-directed TGF emission [7] with higher timing resolution in both desired wavelengths, we are currently developing photometers to install at the TASD site sharing the same field of view as the high-speed video camera and will report on the optical emissions from atmospheric electrical discharge processes that peak at 337 nm (associated with the streamer development) and 777 nm (associated with the stable leader propagation). This will allows us to directly determine if the downward moving TGFs are a variant of the same phenomenon of upward TGFs observed by satellites.

V. ACKNOWLEDGEMENTS

Operation and analyses of this study have been supported by NSF grants AGS-2112709, AGS-1844306, AGS-1613260, AGS-1205727, and AGS-1720600. The Telescope Array experiment is supported by the Japan Society for the Promotion of Science(JSPS)

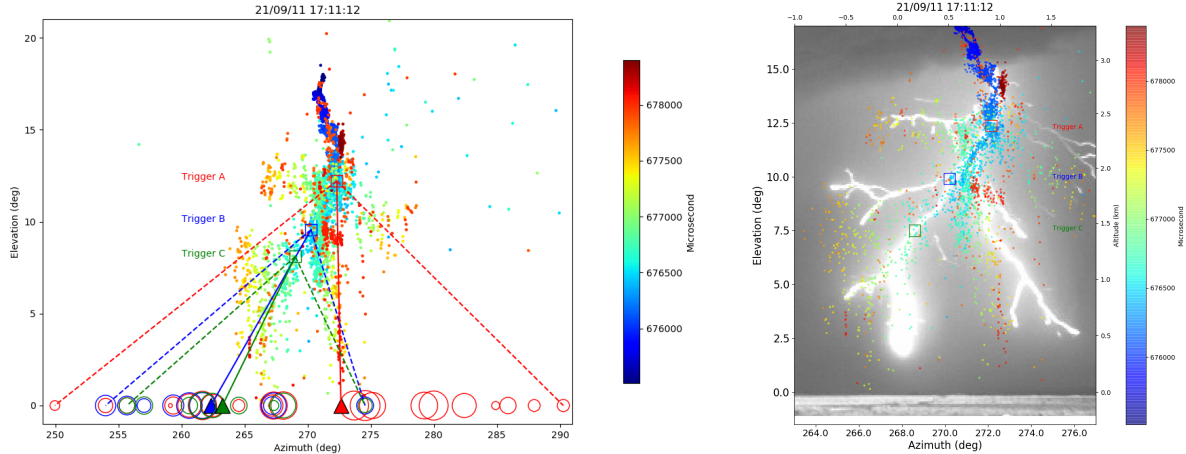


FIG. 1. The fourth flash using the INTF and the TASD detectors (left) and the high-speed video camera in addition to the INTF (right). The left-hand plot shows the elevation vs. azimuth plots of the INTF observations of the fourth flash. The color represents the timing (blue is earlier and red is later in the flash). The dashed lines indicate the possible maximum opening angle of trigger A,B, and C. The red, green, and blue dashed lines point from the source of the TGF for trigger A,B, C and consecutively to the TASD detectors at the edges of the footprint observation on the ground. The circles on the ground refer to the TASD detectors triggered by the TGF observation. The color corresponds to each trigger using the same color code as the dashed lines. The size of each circle is proportional to the energy deposited in the scintillator detector logarithmically. The right-hand plot shows the elevation vs. azimuth for the whole flash in a still image using the high-speed video camera in addition to the INTF point sources using the same color scale as the left-hand plot.

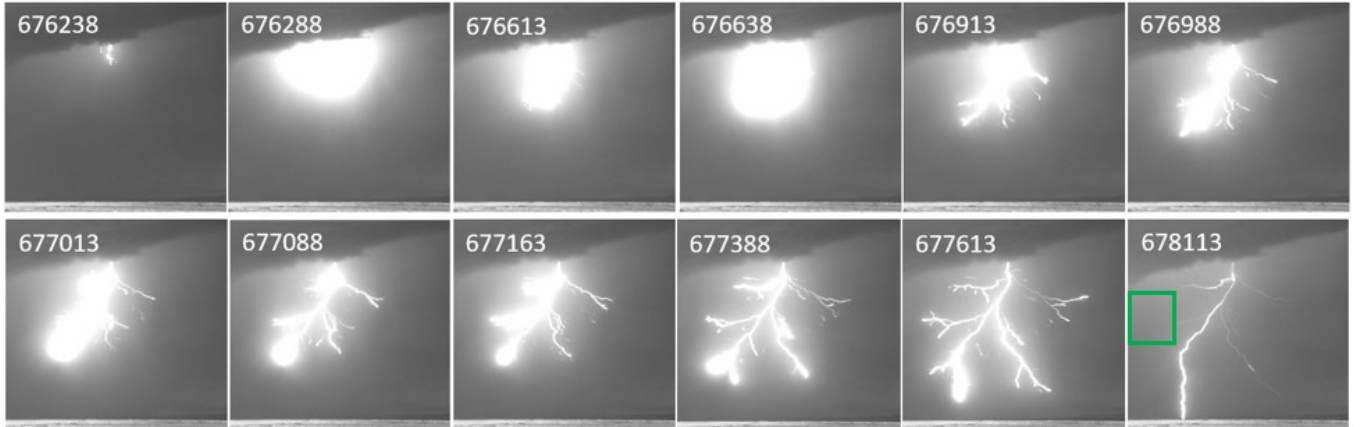


FIG. 2. High speed video still photograph selected images of the fourth TGF producing flash from the time it breaks below the cloud until the return stroke. Note that the time difference between these images does not correspond to the time resolution of the camera. These images are 12 images selected to cover the view of the whole flash. The green square over the last image indicates the area monitored to extract the luminosity variation. The timing in microseconds from the 17:11:12 is displayed at the left corner of each image.

through Grants-in-Aid for Priority Area 431, for Specially Promoted Research JP21000002, for Scientific Research (S) JP19104006, for Specially Promoted Research JP15H05693, for Scientific Research (S) JP15H05741, for Science Research (A) JP18H03705, for Young Scientists (A) JPH26707011, and for Fostering Joint International Research (B) JP19KK0074, by the joint research program of the Institute for Cosmic Ray Research (ICRR), The University of

Tokyo; by the U.S. National Science Foundation awards PHY-0601915, PHY-1404495, PHY-1404502, and PHY-1607727; by the National Research Foundation of Korea (2016R1A2B4014967, 2016R1A5A1013277, 2017K1A4A3015188, 2017R1A2A1A05071429); by the Russian Academy of Sciences, RFBR grant 20-02-00625a (INR), IISN project No. 4.4502.13, and Belgian Science Policy under IUAP VII/37 (ULB). The foundations of Dr. Ezekiel R. and Edna Wattis Dumke, Willard L. Ec-

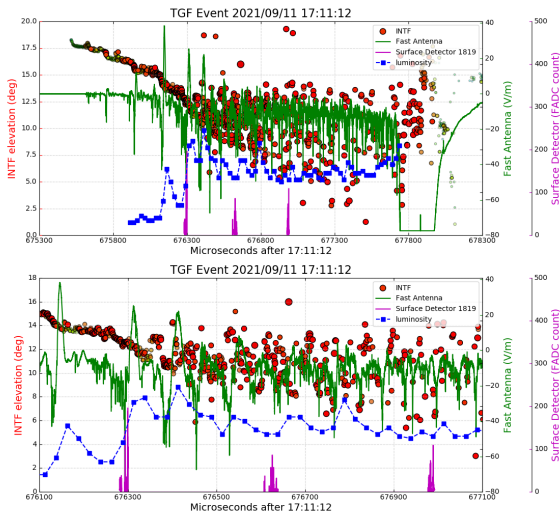


FIG. 3. This figure shows the TASD waveforms in hot pink, the average luminosity vs. time in dark blue, the fast antenna waveform in green, the INTF elevation vs. time in red circles (size and color are proportional to the power of the radio signal). Top: The flash observed from initiation until the first return stroke within 3 ms duration. Bottom: a zoomed in version of the top plot within 1 ms. It shows a clear sequence of the radio, gamma, and optical emission.

cles, and George S. and Dolores Doré Eccles all helped with generous donations. The State of Utah supported the project through its Economic Development Board, and the University of Utah through the Office of the Vice President for Research. The experimental site became available through the cooperation of the Utah School and Institutional Trust Lands Administration (SITLA), U.S. Bureau of Land Management (BLM), and the U.S. Air Force. We appreciate the assistance of the State of Utah and Fillmore offices of the BLM in crafting the Plan of Development for the site. Patrick Shea assisted the collaboration with valuable advice on a variety of topics. The people and the officials of Millard County, Utah have been a source of steadfast and warm support for our work which we greatly appreciate. We are indebted to the Millard County Road Department for their efforts to maintain and clear the roads which get us to our sites. We gratefully acknowledge the contribution from the technical staffs of our home institutions. An allocation of computer time from the Center for High Performance Computing at the University of Utah is gratefully acknowledged. We thank Ryan Said and W. A. Brooks of Vaisala Inc. for providing quality NLDN data lightning discharges over and around the TASD under their academic research use policy.

[1] G. J. Fishman *et al.*, “Discovery of intense gamma-ray flashes of atmospheric origin,” *Science*, vol. 264, p. 1313, 1994.

[2] C. Kouveliotou, “BATSE results on observational properties of gamma-ray bursts,” *The Astrophysical Journal Supplement*, vol. 92, pp. 637–642, June 1994.

[3] T. Gjesteland *et al.*, “A new method reveals more tgf’s in the rhessi data,” *Geophysical Research Letters*, vol. 39, no. 5, 2012.

[4] B. W. Grefenstette *et al.*, “First rhessi terrestrial gamma ray flash catalog,” *Journal of Geophysical Research: Space Physics*, vol. 114, no. A2, 2009.

[5] M. S. Briggs *et al.*, “First results on terrestrial gamma ray flashes from the fermi gamma-ray burst monitor,” *Journal of Geophysical Research: Space Physics*, vol. 115, no. A7, 2010.

[6] M. Marisaldi *et al.*, “Detection of terrestrial gamma ray flashes up to 40 mev by the agile satellite,” *Journal of Geophysical Research: Space Physics*, vol. 115, no. A3, 2010.

[7] N. Ostgaard *et al.*, “First 10 months of tgf observations by asim,” *Journal of Geophysical Research: Atmospheres*, vol. 124, no. 24, pp. 14024–14036, 2019.

[8] M. Stanley *et al.*, “A link between terrestrial gamma-ray flashes and intracloud lightning discharges,” *Geophysical Research Letters*, vol. 33, no. 6, 2006. L06803.

[9] X. Shao *et al.*, “A closer examination of terrestrial gamma ray flash related lightning processes,” *J. Geophys. Res.*, vol. 115, p. A00E30, 2010.

[10] G. Lu *et al.*, “Lightning mapping observation of a terrestrial gamma ray flash,” *Geophys. Res. Lett.*, vol. 37, p. L11806, 2010.

[11] S. A. Cummer *et al.*, “The lightning-tgf relationship on microsecond timescales,” *Geophys. Res. Lett.*, vol. 38, p. L14810, 2011.

[12] S. A. Cummer *et al.*, “Lightning leader altitude progression in terrestrial gamma-ray flashes,” *Geophys. Res. Lett.*, vol. 42, p. 7792–7798, 2015.

[13] F. Lyu *et al.*, “Ground detection of terrestrial gamma ray flashes from distant radio signals,” *Geophysical Research Letters*, vol. 43, no. 16, pp. 8728–8734, 2016.

[14] A. Gurevich, “On the theory of runaway electrons,” *Soviet Phys. JETP*, vol. 12, no. 5, p. 904–912, 1961.

[15] J. R. Dwyer, “Source mechanisms of terrestrial gamma-ray flashes,” *Journal of Geophysical Research: Atmospheres*, vol. 113, no. D10, 2008.

[16] J. R. Dwyer, “A fundamental limit on electric fields in air,” *Geophysical Research Letters*, vol. 30, no. 20, 2003.

[17] S. Celestin and V. P. Pasko, “Energy and fluxes of thermal runaway electrons produced by exponential growth of streamers during the stepping of lightning leaders and in transient luminous events,” *Journal of Geophysical Research: Space Physics*, vol. 116, no. A3, 2011.

[18] J. R. Dwyer and M. A. Uman, “The physics of lightning,” *Physics Reports*, vol. 534, pp. 147–241, Jan 2014.

- [19] G. D. Moss *et al.*, “Monte carlo model for analysis of thermal runaway electrons in streamer tips in transient luminous events and streamer zones of lightning leaders,” *Journal of Geophysical Research: Space Physics*, vol. 111, no. A2, 2006.
- [20] J. R. Dwyer and S. A. Cummer, “Radio emissions from terrestrial gamma-ray flashes,” *Journal of Geophysical Research: Space Physics*, vol. 118, no. 6, pp. 3769–3790, 2013.
- [21] R. Abbasi, T. Abu-Zayyad, M. Allen, E. Barcikowski, J. Belz, D. Bergman, S. Blake, M. Byrne, R. Cady, B. Cheon, *et al.*, “Gamma ray showers observed at ground level in coincidence with downward lightning leaders,” *Journal of Geophysical Research: Atmospheres*, vol. 123, no. 13, pp. 6864–6879, 2018.
- [22] J. Belz, P. Krehbiel, J. Remington, M. Stanley, R. Abbasi, R. LeVon, W. Rison, D. Rodeheffer, T. Abu-Zayyad, M. Allen, *et al.*, “Observations of the origin of downward terrestrial gamma-ray flashes,” *Journal of Geophysical Research: Atmospheres*, vol. 125, no. 23, p. e2019JD031940, 2020.
- [23] T. Abu-Zayyad, R. Aida, M. Allen, R. Anderson, R. Azuma, E. Barcikowski, J. Belz, D. Bergman, S. Blake, R. Cady, *et al.*, “The surface detector array of the telescope array experiment,” *Nuclear Instruments and Methods in Physics Research Section A: Accelerators, Spectrometers, Detectors and Associated Equipment*, vol. 689, pp. 87–97, 2012.
- [24] R. Abbasi, M. Abe, T. Abu-Zayyad, M. Allen, R. Anderson, R. Azuma, E. Barcikowski, J. Belz, D. Bergman, S. Blake, *et al.*, “The bursts of high energy events observed by the telescope array surface detector,” *Physics Letters A*, vol. 381, no. 32, pp. 2565–2572, 2017.
- [25] W. Rison, R. J. Thomas, P. R. Krehbiel, T. Hamlin, and J. Harlin, “A gps-based three-dimensional lightning mapping system: Initial observations in central new mexico,” *Geophysical research letters*, vol. 26, no. 23, pp. 3573–3576, 1999.
- [26] R. J. Thomas, P. R. Krehbiel, W. Rison, S. J. Hunyady, W. P. Winn, T. Hamlin, and J. Harlin, “Accuracy of the lightning mapping array,” *Journal of Geophysical Research: Atmospheres*, vol. 109, no. D14, 2004.
- [27] M. Stock, M. Akita, P. Krehbiel, W. Rison, H. Edens, Z. Kawasaki, and M. Stanley, “Continuous broadband digital interferometry of lightning using a generalized cross-correlation algorithm,” *Journal of Geophysical Research: Atmospheres*, vol. 119, no. 6, pp. 3134–3165, 2014.
- [28] F. Lyu, S. Cummer, and L. McTague, “Insights into high peak current in-cloud lightning events during thunderstorms,” *Geophysical Research Letters*, vol. 42, pp. 1–8, 08 2015.

VI. SUPPORTING INFORMATION

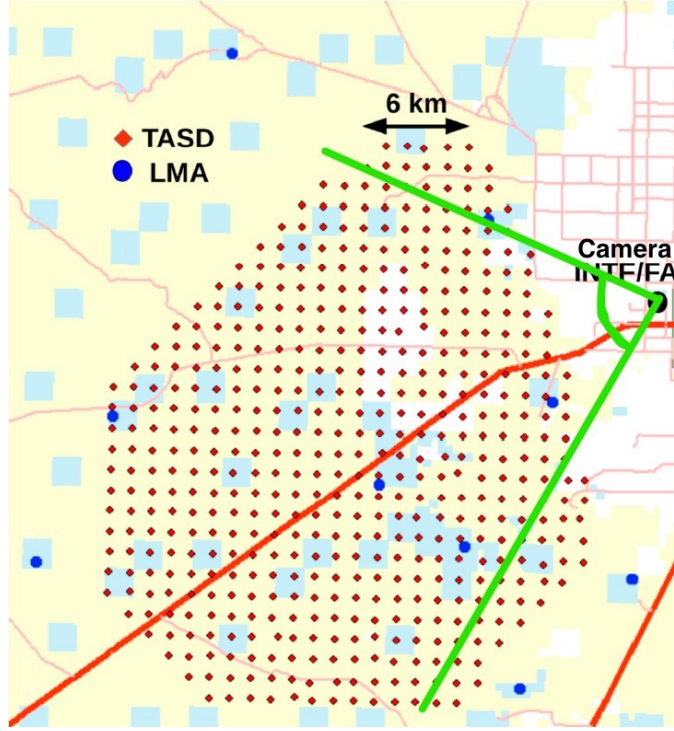


FIG. 4. The layout of the TASD detector and the LMA, in addition to the high-speed video camera, the INTF, and the FA. The Telescope Array Surface Detector (TASD) 507 station, in red diamonds, deployed in the southwestern desert of Utah over a 700 km^2 . While, the Lightning Mapping Array nine stations, in blue circles, deployed throughout the Telescope Array detector. The high-speed video camera, the interferometer and the fast sferic sensor are located ten kilometers to the eastern most edge of the Telescope Array detector. The field of view of the high-speed video camera is demonstrated in the bright green lines with an opening angle of 84 degrees.

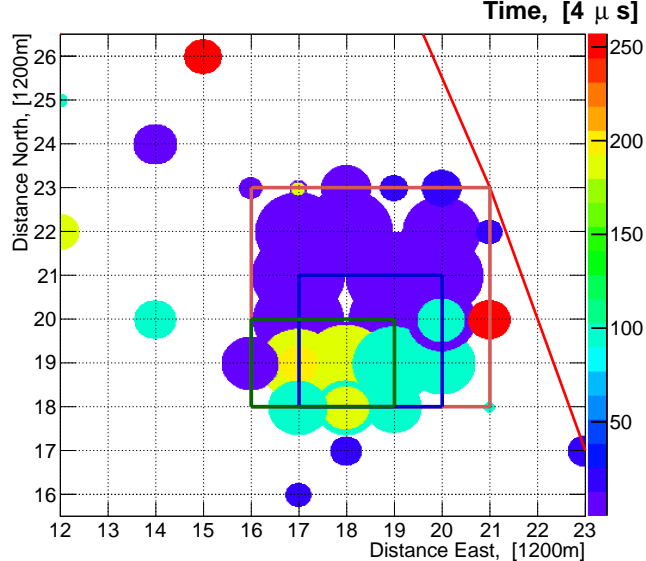


FIG. 5. The TASD footprint including trigger A, trigger B, and trigger C bounded by the red, blue, and green squares consecutively. The grid spacing of the surface scintillators is 1.2 km. The area of each circle is proportional to the logarithm of the energy deposit, and the color indicates relative timing in $4\mu\text{s}$ steps. The red line denotes the eastern border of the TASD array.